

**CALCULATION OF TEMPERATURE REGIMES  
FOR STREAMLINED BODIES  
WITH VARIOUS THERMAL PROPERTIES**

V. I. Zinchenko, V. I. Laeva, and T. S. Sandrykina

UDC 533.526:536.24

Heat exchange occurring in a body at high supersonic velocities can be an effective means for protecting constructions from overheating in regions of maximum heat fluxes, as was noted for steady-state regimes [1, 2]. Analysis [3] of the characteristics of nonstationary conjugate heat exchange for various flow regimes in the boundary layer showed that a large drop in surface temperature can cause not only heat exchange but also blow-in of a cooling gas in regions of high heat loads. The above-mentioned works are concerned with axisymmetric flow around a body. At the same time, of much practical interest is the motion at angles of attack at which the difference between the heat fluxes on the windward and leeward sides can be rather substantial and cause heat transfer in both the lengthwise and circular directions.

In the present paper, we solve the problem of heating and study the influence of heat transfer in a spatial case for materials with various thermal properties. The thermal state for a three-dimensional nonstationary heat-conduction equation is modeled using boundary conditions that correspond to assignment of heat fluxes from the gas phase for spatial supersonic flow around a spherically blunted cone with allowance for the influence of possible blow-in from the surface of a spherically blunted end.

1. To determine temperature fields in a porous spherical casing under the assumption of one-dimensional filtration of blown gas toward the normal to the surface, we write the equation of conservation of energy in the natural coordinate system related to the body axis as

$$\begin{aligned} \pi_{\rho_1} \frac{\partial \theta}{\partial \tau} = & \frac{1}{h_1 r} \left[ \frac{\partial}{\partial n_1} \left( h_1 r \pi_{\lambda_1} \frac{\partial \theta}{\partial n_1} \right) + \frac{\partial}{\partial s} \left( \frac{r}{h_1} \pi_{\lambda_1} \frac{\partial \theta}{\partial s} \right) \right. \\ & \left. + \frac{\partial}{\partial \varphi} \left( \frac{h_1}{r} \pi_{\lambda_1} \frac{\partial \theta}{\partial \varphi} \right) \right] + \frac{(\bar{\rho} \bar{v})_w \sqrt{\text{RePr}} \lambda_{e0} r_w}{h_1 \lambda_*} \frac{r_w}{r} \frac{\partial \theta}{\partial n_1}, \end{aligned} \quad (1.1)$$

$$0 < n_1 < L/R_N, \quad 0 < s < s_1, \quad 0 < \varphi < \pi.$$

For the conical part of the body, the heat-conduction equation in a cylindrical coordinate system has the form

$$\begin{aligned} \pi_{\rho_2} \frac{\partial \theta}{\partial \tau} = & \frac{1}{r} \frac{\partial}{\partial r} \left( r \pi_{\lambda_2} \frac{\partial \theta}{\partial r} \right) + \frac{\partial}{\partial z} \left( \pi_{\lambda_2} \frac{\partial \theta}{\partial z} \right) + \frac{1}{r^2} \frac{\partial}{\partial \varphi} \left( \pi_{\lambda_2} \frac{\partial \theta}{\partial \varphi} \right), \end{aligned} \quad (1.2)$$

$$z_1 < z < z_f, \quad r_{w1} < r < r_w(z), \quad 0 < \varphi < \pi.$$

At the gas flow-body interface, we have

$$\tilde{q}_w \sqrt{\text{RePr}} \frac{\lambda_{e0}}{\lambda_*} - \pi_{\sigma} \theta^4 = - \left( \pi_{\lambda_i} \frac{\partial \theta}{\partial n_1} \right)_w, \quad i = 1, 2; \quad (1.3)$$

on the inner surface of the porous casing,

$$\left( \pi_{\lambda_1} \frac{\partial \theta}{\partial n_1} \right)_{w1} = \sqrt{\text{RePr}} \frac{\lambda_{e0}}{\lambda_*} \frac{r_w}{(r h_1)_{w1}} (\bar{\rho} \bar{v})_w (\theta_i - \theta_{w1}); \quad (1.4)$$

---

Institute of Applied Mathematics and Mechanics, Tomsk 634050. Translated from *Prikladnaya Mekhanika i Tekhnicheskaya Fizika*, Vol. 37, No. 5, pp. 106-114, September-October, 1996. Original article submitted December 15, 1993; revision submitted June 28, 1995.

on the inner surface of the conical part,

$$\pi_{\lambda_2} \frac{\partial \theta}{\partial r} \Big|_{r=r_{w1}} = 0; \quad (1.5)$$

at the sphere-cone interface,

$$\pi_{\lambda_1} \left[ \frac{1}{h_1} \frac{\partial \theta}{\partial s} \frac{1}{\sqrt{1+h_1^2 \tan^2 \beta}} + \frac{h_1 \tan \beta}{\sqrt{1+h_1^2 \tan^2 \beta}} \frac{\partial \theta}{\partial n_1} \right] = \pi_{\lambda_2} \frac{\partial \theta}{\partial z}; \quad (1.6)$$

for  $z = z_f$  the adiabatic condition is

$$\frac{\partial \theta}{\partial z} \Big|_{z=z_f} = 0; \quad (1.7)$$

for flow having a symmetry plane

$$\frac{\partial \theta}{\partial \varphi} \Big|_{\varphi=0} = \frac{\partial \theta}{\partial \varphi} \Big|_{\varphi=\pi} = 0; \quad (1.8)$$

the initial condition is

$$\theta \Big|_{r=0} = \theta_i. \quad (1.9)$$

In (1.1)–(1.9) the linear dimensions are referred to the radius of the blunted end  $R_N$ ;  $\theta = T/T_*$  is the dimensionless temperature;  $h_1 = 1 - n_1$  and  $r = r_w - n_1 \cos \chi$  are the Lamé coefficients for the spherical part;  $(\bar{p}v)_w = (\rho v)_w \sqrt{Re}/(\rho_{e0} v_m)$  is the dimensionless flow rate of the cooling gas;

$$\pi_{\rho_1} = \frac{\rho_1 c_1}{\rho_* c_*} (1 - \Pi) + \frac{\rho_g c_g}{\rho_* c_*} \Pi, \quad \pi_{\lambda_1} = \frac{\lambda_1}{\lambda_*} (1 - \Pi) + \frac{\lambda_g}{\lambda_*} \Pi,$$

$$\pi_{\rho_2} = \frac{\rho_2 c_2}{\rho_* c_*}, \quad \pi_{\lambda_2} = \frac{\lambda_2}{\lambda_*}, \quad \pi_\sigma = \frac{\varepsilon \sigma T_{e0}^3 R_N}{\lambda_*}, \quad \tau = \frac{t}{t_*}, \quad Re = \frac{\rho_{e0} v_m R_N}{\mu_{e0}}$$

are dimensionless parameters;  $t_* = R_N^2 \rho_* c_* / \lambda_*$  is the characteristic time;  $n_1$  is the normal to the external contour of the body;  $\beta$  is the cone half-angle; and  $\tilde{q}_w$  is the dimensionless heat flux from the gas phase which is related to the dimensional value

$$q_w = \frac{\mu_w}{Pr} \frac{\partial H}{\partial n} \Big|_w$$

as  $\tilde{q}_w = q_w \sqrt{Re}/(\rho_{e0} v_m H_{e0})$ , where  $v_m = \sqrt{2H_{e0}}$ ,  $H_{e0}$  is the enthalpy of retardation. The subscripts  $e0$  and  $w$  refer to the conditions on the outer surface of the boundary layer at the retardation point and at the interface between the media  $n_1 = 0$ , respectively,  $w1$  refers to the conditions at the inner contour of the calculation region, 1 and 2 to the characteristics of the condensed phase of the spherical and conical parts; g to the gas phase of the porous casing; asterisk to the characteristic values; and i to the initial temperature.

Note that, in addition to the above boundary conditions in the vicinity of the retardation point of the flow on the spherical part, for Eq. (1.1) we can establish the symmetry conditions in the coordinate system related to the retardation point. To determine the heat flux from the gas phase  $q_w$ , it is necessary to solve the conjugate problem of seeking the characteristics of the spatial boundary layer. In the first stage, however, we use the formulas of [4] for  $q_w(z, \varphi)$  for impermeable bodies, which are in fair agreement with the calculated results of [5]. In this case, in the absence of blow-in from the surface of the blunted end in the turbulent regime, the heat flux on the conical part has the form

$$q_w^0(z, \varphi) = \left( \frac{\alpha}{c_p} \right)^0 (H_r - h_w), \quad \left( \frac{\alpha}{c_p} \right)^0 = \frac{2.2 (p_e/p_{e0})(u_e/v_m)}{k^{0.4} r_w^{0.2}} \frac{16.4 U_\infty^{1.25} \rho_\infty^{0.2}}{R_N^{0.2} (1 + h_w/H_{e0})^{2/3}}, \quad (1.10)$$

where [4]  $u_e/v_m = \sqrt{1 - (p_e/p_{e0})^{(\gamma-1)/\gamma}}$ ;  $k = (\gamma - 1 + 2/M_\infty^2)/(\gamma + 1)$ ;  $H_r = H_{e0}[(p_e/p_{e0})^{(\gamma-1)/\gamma} + \sqrt[3]{Pr}(u_e/v_m)^2]$ ;  $(\alpha/c_p)^0$  [kg/(m<sup>2</sup> · sec)];  $U_\infty$  [km/sec] is the flow velocity;  $\rho_\infty$  [kgf · sec<sup>2</sup>/m<sup>4</sup>] is the flow density;  $R_N$  [m] is the radius of the spherically blunted end; and  $p_e/p_{e0}$  is the pressure distribution on the surface referred to the retardation pressure determined from the results of solution of the spatial gas-dynamic problem [6].

The effect of blow-in on the heat flux in the screen zone on the conical part can be estimated from the results of [7]. In this case, for moderate blows of a homogeneous gas we have

$$q_w(z, \varphi) = \left(\frac{\alpha}{c_p}\right)(H_r - h_w), \quad \left(\frac{\alpha}{c_p}\right) = \left(\frac{\alpha}{c_p}\right)^0 [1 - k_1 b^{k_2}]. \quad (1.11)$$

Here  $k_1$  and  $k_2$  are constants;  $b$  is a dimensionless parameter that characterizes the ratio of the total mass of blown gas to the product of the heat-exchange coefficient in cross-section  $z$  in the absence of blow-in by the surface area of the cone from  $z_1$  to the current value of  $z$ . We write the law of gas-flow rate  $(\rho v)_w$  in the coordinate system  $(s', \varphi', n_1)$  related to the retardation point, for which the flow on the spherically blunted end is axisymmetric, as  $(\rho v)_w(s') = (\rho v)_w(0)(1 + a \sin^2 s')$ . Taking into account the closeness of  $\varphi$  and  $\varphi'$  for the calculated parameters, we obtain

$$b = \frac{2(\rho v)_w(0)[1 - \cos s'_1 + a(2/3 - \cos s'_1 + (1/3) \cos^3 s'_1)]}{(z - z_1)(\cos \beta)^{-1}[2 \sin(\pi/2 - \beta) + \tan \beta(z - z_1)](\alpha/c_p)^0(z, \varphi)}, \quad (1.12)$$

where  $\cos s'_1 = \cos s_1 \cos \alpha + \sin s_1 \cos \varphi \sin \alpha$ ;  $s_1 = \pi/2 - \beta$ ; and  $\alpha$  is the angle of attack. The representation in the form of the second relation in (1.11) for spatial flow was used for the vicinity of the symmetry plane on a windward side [8]. In our case it is extended to the entire side surface, and this requires a more precise definition of the influence of blow-in from the surface of the blunted end on the heat-exchange characteristics in the screen zone. As a whole, Eqs. (1.10) and (1.11) determine the heat load on the conical part of a streamed body within the framework of the above assumptions.

As regards the thermal regime of a porous spherical casing, it has been shown [3] that, with blow-in of a gas, a steady-state regime is rapidly established on the porous part for constant retardation parameters. As the flow rate of the cooling gas increases, the temperature of the spherically blunted end becomes lower than that of the conical part, i.e., there is heat transfer from the conical to the spherical part. To model this process and to estimate the effect of heat transfer in the conjugation region, we imposed two conditions at the interface between the spherical and conical parts ( $z = z_1$ ): the adiabatic condition and the condition of a given temperature that coincided with the initial cooling gas temperature in the casing cavity

$$\left.\frac{\partial \theta}{\partial z}\right|_{z=z_1} = 0 \quad \text{or} \quad \theta\Big|_{z=z_1} = \theta_i. \quad (1.13)$$

The boundary problem was solved numerically by the method of splitting using the implicit difference schemes obtained by the iteration-interpolation method of [9, 10]. The initial calculation grid consisted of  $31 \times 61 \times 6$  points in the  $r$ ,  $z$ , and  $\varphi$  directions. A twofold concentration of points in the  $\varphi$  coordinate caused a difference in the surface temperature not greater than 2%. In the solution of the problem, the time step was variable and its value was determined by assignment of a surface-temperature rise. Iterations were performed in each time layer, because of the nonlinearity of balance conditions (1.3). From 300 to 1600 calculated time layers were required to enter a steady-state regime. This number was determined by the heat flux and the thermal properties of the material.

2. In numerical integration the cone half-angle is  $\beta = 5^\circ$ , the radius of the blunted end is  $R_N = 1.85 \cdot 10^{-2}$  m,  $z_f = 5.2$ , and  $r_{w1} = 0.22$ . The flow parameters were constant:  $\rho_\infty = 0.02$  kgf  $\cdot$  sec<sup>2</sup>/m<sup>4</sup>, and  $U_\infty = 2.078$  km/sec, which corresponds to Mach number  $M_\infty = 6$ . In this case, the retardation enthalpy  $H_{e0} = 2.46 \cdot 10^6$  m<sup>2</sup>/sec<sup>2</sup>, and the angle of attack  $\alpha = 20^\circ$ . The Reynolds number obtained from the retardation parameters is  $Re = \rho_{e0} \sqrt{2H_{e0}} R_N / \mu_{e0} \approx 0.7 \cdot 10^6$ , which is responsible for the turbulent flow regime in the boundary layer on the conical part of the body. The thermal properties of the conical part were constant. The heat-conductivity coefficient varied over a wide range:  $\lambda_2 = 10$ –380 W/(m  $\cdot$  K). As base materials we used steel [ $\lambda_2 = 20$  W/(m  $\cdot$  K),  $c_2 = 600$  J/(kg  $\cdot$  K), and  $\rho_2 = 7800$  kg/m<sup>3</sup>] and copper [ $\lambda_2 = 380$  W/(m  $\cdot$  K),  $c_2 = 386$  J/(kg  $\cdot$  K) and  $\rho_2 = 8930$  kg/m<sup>3</sup>]. The initial temperature was  $T_i = 300$  K and  $\varepsilon = 0.85$ .

Figure 1 shows the distributions of heat fluxes  $q_w$  and surface temperature  $T_w$  along the  $z$  coordinate in various meridional cross-sections [curves 1–3 correspond to the windward side of the symmetry plane ( $\varphi = 0$ ), and curves 1'–3' correspond to the leeward side ( $\varphi = \pi$ )] for a steel specimen for  $(\rho v)_w = 0$ . The calculations were performed using the boundary conditions of the first kind from (1.13) up to the moment the process

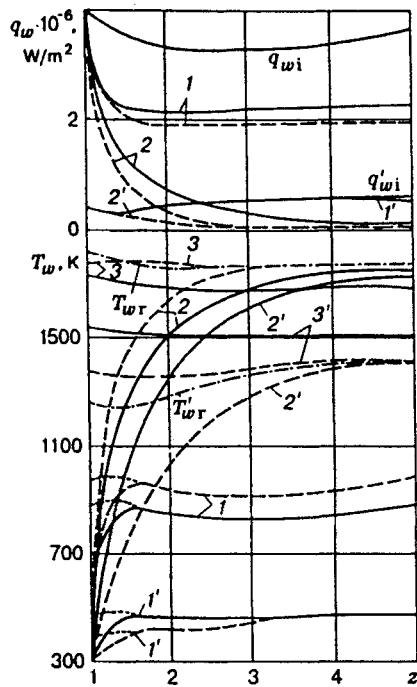


Fig. 1

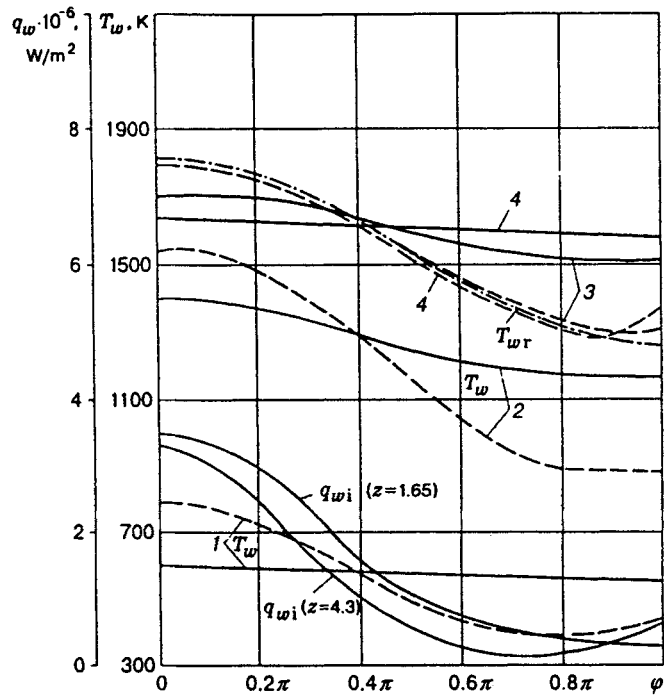


Fig. 2

entered a steady-state regime. Curves 1 and 1' correspond to  $t = 5$  sec, and curves 2 and 2' to the steady-state regime. Curves 3 and 3' also correspond to the steady-state regime, but in this case adiabatic condition (1.13) was used. In addition to the three-dimensional calculations (solid curves), the two-dimensional problem following from (1.2) was solved along various cross-sections  $\varphi$  (dashed curves) to estimate the influence of heat transfer in the circular direction. The dashed-dotted curves denote the distributions of the radiation-balance temperature in the symmetry plane on the windward and leeward sides. This temperature was determined from the condition of conservation of energy

$$\tilde{q}_w \sqrt{\text{Re Pr}} \frac{\lambda_{e0}}{\lambda_*} = \pi \sigma \theta_w^4 \quad (2.1)$$

The distribution of heat fluxes at  $T_i = 300$  K (curves  $q_{wi}$  and  $q'_{wi}$  for  $\varphi = 0, \pi$ ) shows that the heat load varies substantially along the circular coordinate, and this causes heat transfer from the windward to the leeward side. The solution taking into account the heat flux in the circular direction gives much higher temperature values on the leeward side (by more than 300 K for  $t \rightarrow \infty$ ) than the solution of the two-dimensional problem. At the same time, the surface temperature of the most heat-stressed part for  $\varphi = 0$  decreases by more than 100 K for  $1.5 < z < 3$ . As should be expected, a substantial stratification of the surface temperatures occurs on the windward and leeward sides at times that are close to the initial time in the solution of the three-dimensional problem (curves 1 and 1'). When the steady-state regime is established, the difference in  $T_w$  in the symmetry plane of the flow does not exceed 250 K for the region adjoining the spherical fore end. On the back part of the conical surface, the difference in surface temperatures is not greater than 20 K. With distance from the fore end, the values of  $T_w$  for  $\varphi = \pi$  exceed considerably (due to the heat transfer to the leeward side) the radiation-balance temperature  $T'_{wr}$ , which determines the highest possible surface temperature in the absence of heat flux in the longitudinal and circular directions.

It is interesting to analyze the boundary condition at the joint of the spherical and conical parts. Curves 1 show that initially the effect of the given boundary conditions for  $z = z_1$  is localized within a fairly narrow region adjoining  $z_1$  and does not manifest itself on the major part of the conical surface (curves 1 continued by points were obtained for the adiabatic condition for  $z = z_1$ ). As  $t \rightarrow \infty$ , the resulting values of

the stationary surface temperature (solid and dashed curves 3 and 3') satisfy the expressions

$$\int_{s_1}^{s_f} \int_0^\pi r_w \left[ \frac{\alpha}{c_p} (H_r - h_w) - \varepsilon \sigma T_w^4 \right] ds d\varphi = 0; \quad (2.2)$$

$$\int_{s_1}^{s_f} r_w \left[ \frac{\alpha}{c_p} (H_r - h_w) - \varepsilon \sigma T_w^4 \right] ds = 0 \quad (2.3)$$

for the three- and two-dimensional cases, respectively, which can be readily obtained by integrating the heat conduction equation written for the conical part in the intrinsic coordinate system. Calculations were also performed for  $\lambda_2 \rightarrow \infty$ , which leads to equalization of the temperature field in the streamlined-body material. The temperature values are in good agreement with the results of calculations by the formulas following from (2.2) and (2.3) using the expression for the heat flux

$$q_w(s, \varphi) = \left( \frac{\bar{\alpha}}{c_p} \right) (H_{e0} - c_p T_w), \quad \frac{\int_{s_1}^{s_f} \int_0^\pi r_w (\bar{\alpha}/c_p) ds d\varphi}{\pi \int_{s_1}^{s_f} r_w ds} (H_{e0} - c_p T_w) = \varepsilon \sigma T_w^4; \quad (2.4)$$

$$\left( \int_{s_1}^{s_f} r_w \left( \frac{\bar{\alpha}}{c_p} \right) ds / \int_{s_1}^{s_f} r_w ds \right) (H_{e0} - c_p T_w) = \varepsilon \sigma T_w^4. \quad (2.5)$$

For the given case, when solving the three-dimensional problem, we have  $T_w(s, \varphi) = 1604$  K, and, ignoring the heat transfer in the circular direction,  $T_w(s, 0) = 1790$  K and  $T_w(s, \pi) = 1388$  K.

We note that formula (2.1) characterizes the radiation-balance temperature  $T_{wr}$  in the absence of heat flux to the c-phase, which is usually regarded as the maximum possible temperature. This follows from the above statement of the problem assuming the one-dimensionality of the process for  $t \rightarrow \infty$  when the temperature field in material is equalized. As a result of heat exchange,  $T_w$  can be much higher than  $T_{wr}$  on the leeward side, as follows from Fig. 1 and analysis of formulas (2.2)–(2.5).

Figure 2 shows the effect of the material of the conical part. In the cross-section  $z = 1.65$ , the distributions of the stationary surface temperature along the circular coordinate are presented for copper (curves 1) and steel (curves 2) with the boundary conditions of the first kind from (1.13). Curves 3 and 4 (for copper and steel, respectively) were obtained for the stationary temperature under adiabatic conditions for  $z = z_1$ . The dashed curves correspond to the absence of heat exchange in the circular direction, and the dashed-dotted curve refers to the radiation balance temperature of the wall  $T_{wr}$ . The figure also shows initially, the behavior of the heat flux  $q_{wi}(\varphi)$  in the various  $z$  cross-sections at the initial moment, which leads to the nonmonotonic behavior of dashed curve 4 for  $T_w$ , versus the circular coordinate  $\varphi$ , which also follows from analysis of formula (2.5). Figure 2 shows that use of a better heat-conducting material decreases significantly (to 800 K) the temperature of the streamlined body under the boundary conditions of the first kind which model the heat removal to the spherical part of the body.

The curves in Figs. 2 and 3 show the dynamics of surface-temperature fluctuations in the cross-section  $z = 1.65$  versus the time of the process. Evidently, under the boundary conditions of the first kind for  $z = z_1$  for a poorer heat-conducting material (for steel, curves 2, 2' for the windward and leeward sides in the plane of symmetry) the times of transition to the steady-state regime increase considerably compared with those for a better heat-conducting material (copper, curves 1 and 1'). Neglect of the heat exchange in the circular direction has little effect on the times of attainment of the stationary temperature (dashed curves 1 and 1'). Curves 3 and 3' obtained for steel under adiabatic conditions for  $z = z_1$  show that the form of conditions (1.13) also has a weak effect on the times of attainment of a steady-state regime.

Figure 4 shows the effect of blow-in from the surface of the spherically blunted end for  $(\rho v)_w(0) = 3$  kg/(m<sup>2</sup> · sec),  $a = 9$ ,  $k_1 = 0.285$ , and  $k_2 = 0.165$ . In this case, as in the previous figures, curves 1 and 1' corresponding to the stationary temperature  $T_w$  were obtained for copper; curves 2 and 2' were obtained for

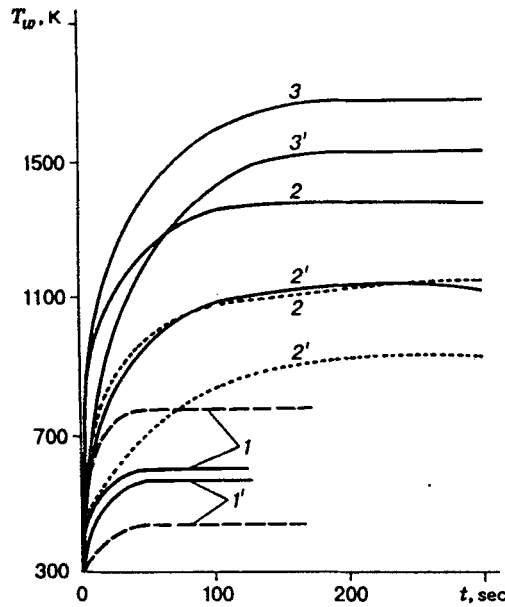


Fig. 3

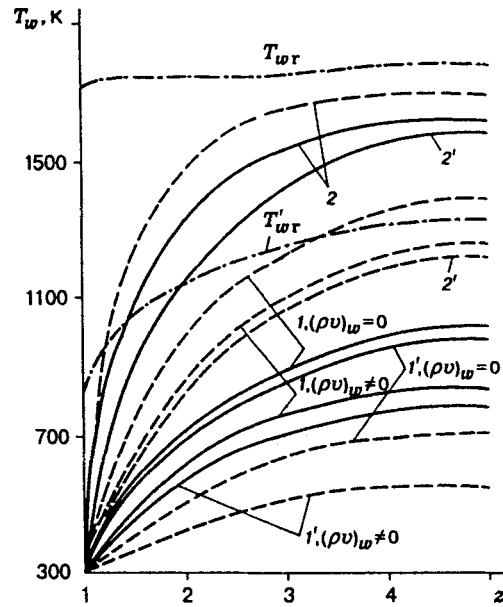


Fig. 4

steel. For  $z = z_1$ , the boundary condition of the first kind was used. As should be expected, a decrease in the heat flux in the screen zone causes a drop in the surface temperatures of the conical part and also in the maximum radiation-balance temperature for  $\varphi = 0$ . Comparison of curves 1 and 1' obtained with and without blow-in, and also of curves 2 and 2' with the corresponding curves in Fig. 1, shows that blow-in of the gas causes a greater stratification of the temperature curves  $T_w(z)$  for  $\varphi = 0, \pi$ . This is caused by the behavior of the heat flux  $q_w(\varphi)$  due to the entry of a large mass of the cooling gas into the leeward side of the conical part. This, in turn, will cause an increase in the role of heat transfer in the circular direction with increasing angles of attack. The gas blow-in from the surface of the spherically blunted end also leads to a monotonic increase in the heat flux  $q_w$  in the screen zone of the conical part in all meridional cross-sections in contrast to the data in Fig. 1 [8]. This increases the heat flux along the  $z$  coordinate in the peripheral regions. Therefore, dashed curves 2 and 2' lie below the radiation-balance temperature values.

Comparison of curves 2, 2' in Fig. 3 [dashed curves 2 and 2' were obtained for  $(\rho v)_w \neq 0$ ] shows that the dynamics of surface-temperature fluctuations in the presence of blow-in is close to the behavior of the corresponding curves without blow-in.

The effect of heat transfer on the maximum surface temperatures in the vicinity of the symmetry plane on the windward and leeward sides (curves 1 and 1') is generalized in Fig. 5 for various materials at a given gas temperature in the cross-section  $z = z_1$ . As above, the dashed curves were constructed ignoring the heat transfer in the circular direction. Figure 5a corresponds to the absence of blow-in from the spherically blunted end, and Fig. 5b to  $(\rho v)_w \neq 0$ . The quantity  $1/S = (\sqrt{\text{RePr}}(\lambda_{e0}/\lambda_*)^{-1}$  expresses the ratio of the conductive to convective heat fluxes,  $T_* = T_i = 300$  K, and the black triangle and black circle correspond to the calculations for various values of the conjugation parameter.

As one might expect, on the windward side ( $\varphi = 0$ ) the dependence of  $\theta_{w\text{max}}$  on  $1/S$  is of a monotonic decreasing character. As the heat conductivity coefficient increases, neglect of the heat exchange in the circular direction overestimates the level of maximum temperatures by a factor of 1.5. On the leeward side ( $\varphi = \pi$ ), allowance for the heat exchange in the circular direction changes the qualitative character of the curve and leads to a considerable increase in the level of maximum temperatures for various materials. Figure 5 shows that the blow-in decreases considerably the maximum temperatures of the body. However, the larger decrease in  $\theta_{w\text{max}}$  is caused by the use of heat-conducting materials.

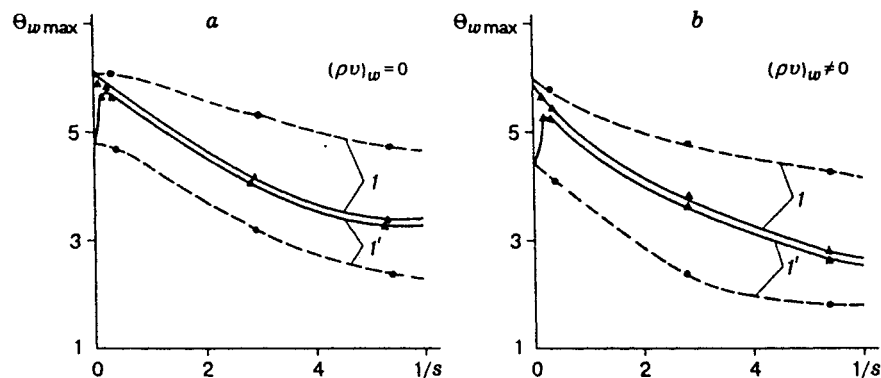


Fig. 5

Thus, we studied the effect of the thermal properties of materials on the temperature fields in a body by assigning the heat flux from the gas phase with and without blow-in from the surface of the spherically blunted end. We considered the change of  $\lambda_2$  from the value  $\lambda_2 = 0$ , which corresponds to the radiation balance temperature  $T_{wr}(z, \varphi)$ , to the value  $\lambda_2 \rightarrow \infty$ , at which formulas for determining the stationary isothermal temperatures were derived. The influence of heat transfer was studied in a spatial case for a series of materials. It was demonstrated that the blow-out of a cooling gas causes a drop in the maximum surface temperature due to the weakening of the heat flux in the screen zone. However, a larger effect is obtained by using highly conducting materials, which ensure a strong heat removal toward the porous spherically blunted end.

To conclude, the authors are very grateful to V. D. Gol'din for the results of gas-dynamic calculations.

This work was supported by the Russian Foundation for Fundamental Research (Grant 93-01-17286).

## REFERENCES

1. V. A. Bashkin and S. M. Reshet'ko, "On maximum temperature of the blunted end with allowance for heat conductivity," *Uch. Zap. TsAGI*, **20**, No. 5, 53-59 (1989).
2. V. A. Bashkin and S. M. Reshetko, "Temperature regime of blunted wedges and cones in supersonic flow with allowance for heat conduction of a wall material," *Uch. Zap. TsAGI*, **21**, No. 4, 11-17 (1990).
3. V. I. Zinchenko, A. G. Kataev, and A. S. Yakimov, "Investigation of the temperature regimes of bodies immersed in flow with surface blowing," *Prikl. Mekh. Tekh. Fiz.*, No. 6, 57-64 (1992).
4. B. A. Zemlyanskii and G. N. Stepanov, "On the calculation of heat exchange in spatial hypersonic air flow around blunted thin cones," *Izv. Akad. Nauk SSSR, Mekh. Zhidk. Gaza*, No. 5, 173-177 (1981).
5. V. I. Zinchenko and O. P. Federova, "Study of a three-dimensional turbulent boundary layer with allowance for a coupled heat exchange," *Prikl. Mekh. Tekh. Fiz.*, No. 3, 118-124 (1989).
6. V. A. Antonov, V. D. Gol'din, and F. M. Pakhomov, *Aerodynamics of Bodies with Blow-in*, Izd. Tomsk Univ., Tomsk (1990).
7. V. N. Kharchenko, "Heat exchange in a hypersonic turbulent boundary layer in cooling gas blow-in through a gap," *Teplofiz. Vys. Temp.*, No. 1, 101-105 (1972).
8. A. V. Bureev and V. I. Zinchenko, "Calculation of the flow field past spherically blunted cones in the vicinity of a plane of symmetry for various shock layer flow regimes with insufflation of gas from the surface," *Prikl. Mekh. Tekh. Fiz.*, No. 6, 72-78 (1991).
9. A. M. Grishin, V. N. Bertzun, and V. I. Zinchenko, *Iteration-Interpolation Method and Its Applications*, Izd. Tomsk Univ., Tomsk (1981).
10. A. M. Grishin, G. G. Tivanov, and A. I. Cheprasov, "Mathematical modeling of the thermal states of axisymmetric bodies of arbitrary cross-section with anisotropic inclusions," in: *Numerical Methods of Continuum Mechanics* [in Russian], **15**, No. 6 (1984), pp. 41-58.